SINGLE SPIKE EXPERIMENTS WITH THE SPARC SASE FEL

I. Boscolo, F.Castelli, S. Cialdi, V. Petrillo, Università di Milano, Milano (Italy)
A.Bacci, L.Serafini, INFN, Milano (Italy)
M. Boscolo, M. Ferrario, C. Vaccarezza, LNF, INFN, Frascati (Italy)
L. Giannessi, C. Ronsivalle, ENEA Frascati, (Italy)
L. Palumbo, M. Serluca, Università La Sapienza Roma (Italy)
G. Andonian,E. Hemsing, G. Marcus, S. Reiche, J. Rosenzweig. UCLA, LA (USA)

Abstract

The single spike operation regime has been analysed in the case of the SPARC injector and free-electron-laser. Various beams at 50 pC and at 1 nC are studied, with different production conditions and performances.

INTRODUCTION

In the FEL emission two different regimes occur depending on the length L_b of the beam.

If the L_b is larger than 2π times the cooperation length L_c, the radiation presents a longitudinal structure constituted by several chaotic peaks, while, if the length of the beam is shorter than $2\pi L_c$, the emission produces a radiation pulse shaped in one single spike [1]. This regime occurs because the radiation emitted by the electrons, travelling from the tail towards the head of the beam, covers all the distance inside the bunch in a time shorter than few gain times, correlating all the particles. The properties of this regime are well-known in 1d: however, the study of single-spike ultra-short radiation in the X rays range [2], as well as in the visible light [3], by means of start-to-end simulations from the photocathode to the end of the undulator, has shown that transverse and non-homogeneity effects due to radiation diffraction and to non–ideal characteristics of the electron beam such as emittance and energy spread change considerably the properties of the emission process. A fundamental problem is also how to produce a suitable beam. In the second part of this paper, the analysis of the 3d scaling law is presented. Then we present some numerical start-to-end FEL simulations made in the case of the SPARC FEL, for some different beam regimes at 50 pC and at 1 nC. The performance of the various bunches are compared and the most interesting of them are discussed.

SCALING LAW

The single spike operation requires that the beam length L_b satisfies the following requirement:

$$L_b \leq 2\pi L_c \qquad (1)$$

with $L_c=L_{c1d}(1+\eta)$

where: $L_{c1d}=\lambda/(\sqrt{3}\,4\pi\rho)$ and η is defined as in [4] :

$$\eta = 0.45\eta_d^{0.57} + 0.55\eta_\varepsilon^{1.6} + 3\eta_\gamma^{2} + 0.35\eta_\varepsilon^{2.9}\eta_\gamma^{2.4} + 51\eta_d^{0.95}\eta_\gamma^{3} + 5.4\eta_d^{0.7}\eta_\varepsilon^{1.9} + 1140\eta_d^{2.2}\eta_\varepsilon^{2.9}\eta_\gamma^{3.2}, \qquad (2)$$

with $\eta_d = L_{g1d}\lambda/(4\pi\sigma_x^2)$ term that accounts for radiation diffraction, $\eta_\varepsilon = \frac{4\pi L_{g1d}\varepsilon_{n,x}^2}{\sigma_x^2\gamma^2\lambda}$ for the emittance and $\eta_\gamma = 4\pi\frac{L_{g1d}}{\lambda_u}\frac{\delta\gamma}{\gamma}$ for the energy spread effects. In these last expressions $L_{g1d}=\lambda_u/(\sqrt{3}\,4\pi\rho)$ is the 1d gain length, $\varepsilon_{n,x}$ the normalized transverse emittance, $\delta\gamma/\gamma$ the energy spread and λ is the radiation wavelength given by the resonance condition $\lambda = \frac{\lambda_u(1+a_w^2)}{2\gamma^2}$.

The FEL parameter ρ, in terms of the beam average current I, of the radial r.m.s dimension σ_x of the beam, of the undulator parameter $K_0=\sqrt{2}\,a_w$ and period number $k_u=2\pi/\lambda_u$, of the Lorentz factor of the beam γ can be written as:

$$\rho = \left[\frac{1}{16}\frac{I}{I_A}\frac{K_o^2[JJ]^2}{\gamma^3\sigma_x^2k_u^2}\right]^{1/3} \qquad (3)$$

where I_A=17 KA is the Alfven current and JJ =$(J_0(\xi)-J_1(\xi))$, J's are Bessel function of argument $\xi = \frac{a_w^2}{2(1+a_w^2)}$.

In (3) the current I is defined as $I=cQ/L_b$ with L_b the whole beam length if the beam current is flat top, or $L_b=\sqrt{2\pi}\sigma_z$ with σ_z the FWHM length, if the longitudinal beam profile is Gaussian.

The single spike condition is:

$$L_b=2\pi L_{c1d}(1+\eta) \qquad (4)$$

and the Q vs L_b scaling law becomes

$$Q = \left(\frac{\pi^2 I_A}{3\sqrt{3}c}\right)\left(\frac{\lambda_u(1+a_w^2)^3}{K_0^2[JJ]^2}\right)\left(\frac{\sigma_x^2}{L_b^2\gamma^3}\right)(1+\eta)^3 \qquad (5)$$

where in the factor η a further irrational dependence on I is contained.

The solution of (5) for four different beams obtained with four different beam lines at 50 pC is presented in Fig 1. The beams present different values of emittance, energy

spread, current profile, longitudinal width and transverse dimension. Their position in the Q vs σ_z plane is represented by green stars in Fig 1, together with single spike operation curves at different σ_x.

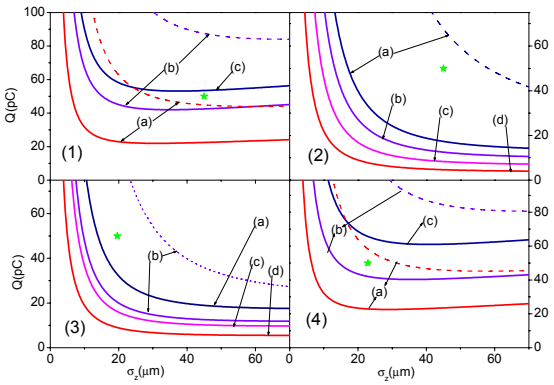

Figure 1:single spike scaling law: solid: 1 spike, dashed: 2 spikes for: (1) beam 1 (a) σ_x=50 μm, (b) σ_x=100 μm (c) σ_x=126 μm. (2) beam 2 (a) σ_x=200 μm (b) σ_x=150 μm (c) σ_x=104 μm, (d) σ_x=50 μm. (3) beam 3: (a) σ_x=150 μm,(b) σ_x=100 μm (c) σ_x=80 μm (d) σ_x=50 μm. (4): beam 4 (a) σ_x=150 μm, (b) σ_x=100 μm, (c) σ_x=50 μm.

Table 1

beam	ϕ(°)	$\varepsilon_{x,n}$ μm	ΔE/E %	σ_z μm	I_{peak} A
1	-84.5	0.47	0.235	45	120
2	-95	0.45	0.069	45	120
3	-89.9	0.63	0.097	20	300
4	-91.4	2.	0.21	22.8	430

OPERATION AT 50 pC

Four different beams generated and driven in the SPARC line [5] have been analysed, characterized substantially by different values of the injection angle ϕ in the first accelerating structure. The RF compression method has been used. The phase spaces together with the current profile are presented in Fig 2. The first beam (fig. 2, window (1)) has been obtained in the standard SPARC operation regime, scaling the parameters from the 1 nC working point by means of the scaling law at the cathode $\sigma_{xyz} \sim Q^{1/3}$ [6], and using therefore a laser pulse length of σ_t=1 psec, illuminating a region of R=0.4 mm. The injection angle ϕ was -84.5°. The beam was compressed at σ_z =45 μm, with a peak current of 120 A. The simulations of the beams 1, 2 and 4 was done with Parmela [7], while case 3 was simulated by ASTRA [8].
Beam (2) was obtained in the blow out regime with a laser pulse of 0.2 psec and an injection angle of -95° in the over-compression condition. The final beam length is again 45 μm and the peak current 120 A, but the energy spread and the transverse dimension are smaller and the current has a different shape.

The last two beams (beam (3), shown in Fig. 2 , window (3) and beam (4), Fig. 2, window (4)) have been injected around the maximum compression phase (respectively -89.9° and -91.4°), obtaining more peaked currents. The difference between them is that beam (3) has been optimized with the genetic algorithm [9], leaving free the intensities of the 12 magnetic coils of the first structure and the injection angles in the last two structures (respectively -34.9° and -2.8). These adjunctive degrees of freedom have permitted to obtain a current very much larger than the first two cases, only a bit smaller than case (4), but with a better control of emittance and of energy spread. The last beam (4) belongs to the high current operation regime, explained in Ref [3].

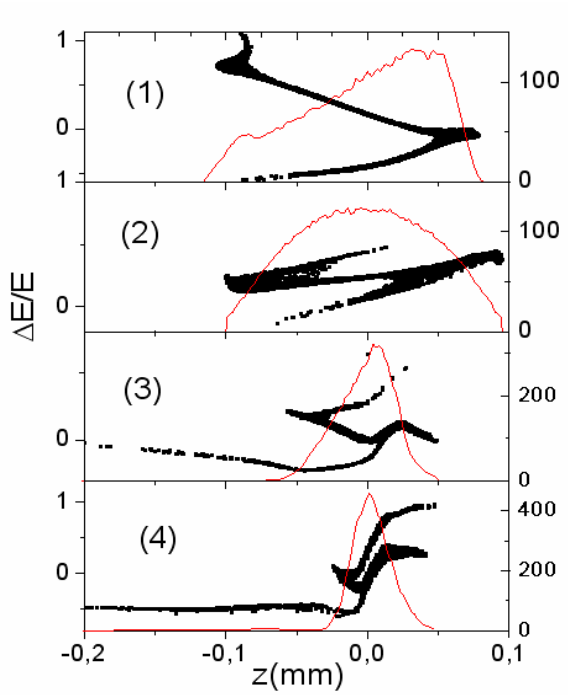

Figure 2: Left axis: Phase space ΔE/E in % vs z (mm) . Right axis: current (a) vs z (mm) for (1): beam 1, (2) beam 2, (3) beam 3 and (4) beam 4.

In table 1 the different characteristics of the beams are summarized. In the last two cases the effect of the large longitudinal space charge forces is that of prevent the complete overcompression, the particles being pushed forward by the electric repulsive forces applied by the slices behind. The result is a folding in the phase space in correspondence of the maximum density with inversion of the energy phase correlation.
The optimum focusing condition for the four beams has been deduced by the scaling law shown in Fig. 1. Values of σ_x and σ_x leading to the single spike operation with the maximum focalization (corresponding to the maximum energy extraction) have been used. For the beam (1) the condition of single spike occurs for σ_x=100 μm. In fact in Fig 1 (1) the green star is positioned near curve (b) solid line (1 spike, and σ_x=100 μm) and well above curve (b) dashed line (2 spikes, σ_x=100 μm). As the beam at 12

meter has σ_x=126 μm, it has been transversally matched to the undulator entrance by means of the SPARC transfer line constituted by two triplets far 3.8 m. The second beam has σ_x=104 μm, so it can be not focused, because exits from the linac with transverse dimensions near to the single spike condition. Beam 3 presents σ_x=79 μm at 12 m, so it has to be matched, as well as beam 4 that exits from the linac with σ_x=208 μm.

The undulator and lattice characteristics are: 6 undulator section of 2.15 m, λ_u=2.8 cm, a_w=1.51, dB/dz=8. T/m. Radiation with wavelength of 500 nm is produced.

In table 2 the most significant radiation characteristics are presented for various values of σ_x. The FEL simulations have been done with GENESIS 1.3 [10] .

Table 2: Radiation Properties: N_{sp}: number of radiation spikes, E: total energy of the pulse, div: radiation divergence, σ^{z}_{rad} :radiation length, bw: normalized bandwidth

beam	σ_x μm	N_{sp}	P_{max} GW	E μJ	div mrad	σ^{z}_{rad} μm	bw %
1	104	1-2	0.13	23	1.7	30	1
	50	1-3	0.095	30	1	70	1
2	104	1-2	0.037	10	0.7	50	0.8
	50	3	0.09	30	0.6	250	1
3	104	1	0.16	16.7	1	20	1
	79	1-2	0.32	44	1	40	1
	50	3	0.37	56	0.9	60	0.8
4	125	1	0.41	39.6	1.2	15	1.1
	100	1-2	0.7	50.8	2	20	1.2
	70	1-2	0.8	68.4	1.6	25	1.3

In figures 3 and 4 the radiation evolution is presented in the plane z(m) vs s (μm), together with the pulse shape P (W) vs s at 11 meter in the undulator. The cases presented are: beam (1), σ_x =104 μm, and beam (4) , σ_x =125 μm. As shown, the predictions of the scaling law are respected. The analysis shows that there is large margin of choice in the single spike operation. The maximum compression regime leads to minima pulse lengths, large peak power and total energy. However, the operation in this regime requires a tight control of the beam line elements (as for instance the magnetic field intensity in the coils of the first structure) and of the injection angles for avoiding the formation of tails that degrade the beam quality and for controlling emittance and energy spread. These last quantities are not demanding for the single spike occurrence, but determine some of the pulse characteristics as, for instance, the divergence and the spectrum.

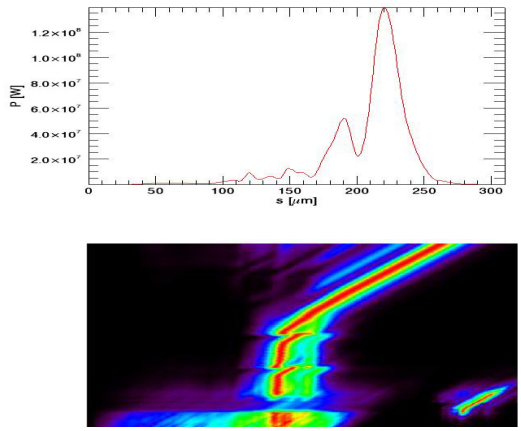

Figure 3: beam 1, σ_x =104 μm: pulse shape P (W) vs s(μm) at 11m. Normalized level curves in the plane z(m) vs s (μm).

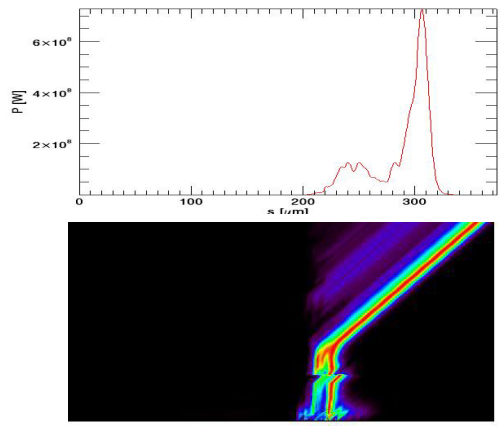

Figure 4: beam 4, σ_x =100 μm: pulse shape P (W) vs s(μm) at 11 meterr. Normalized level curves in the plane z(m) vs s (μm).

OPERATION AT 1 NC

The genetic algorithm has been used for generating a compressed beam at 1 nC. The injection angle in the three accelerating structures, as well as the magnetic intensity in the coils of the first two structures have been left free. In this case the velocity bunching is made in the first two structures. The genetic algorithm has converged on a solution, producing a beam whose phase space is shown in Fig. 5. The evolution of envelope, emittance and the magnetic field profile along the 12 meters of beam line are presented in Fig. 6. The beam has been focused at 100 μm of radius, a focussing channel in the undulator with dB/dz=4 T/m has been used.

Table 3: Properties of the High Charge Beam

$\phi(°)$	$\varepsilon_{x,n}$ μm	$\Delta E/E$ %	σ_z μm	I_{peak} kA
-89.5	1.52	0.078	74	2.6

Table 4: Properties of the Radiation in the High Charge Operation Regime

σ_x μm	N_{sp}	P_{max} GW	E mJ	Lsat (m)	div mrad	$\sigma^{z,}_{rad}$ μm	bw %
100	1-2	7.5	1.4	10	0.7	20	2

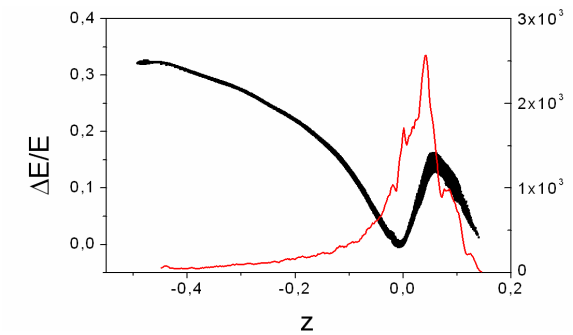

Figure 5 : Left axis: ΔE/E (%) vs z (mm) for the beam at high charge. Right axis: Current(A) vs z(mm).

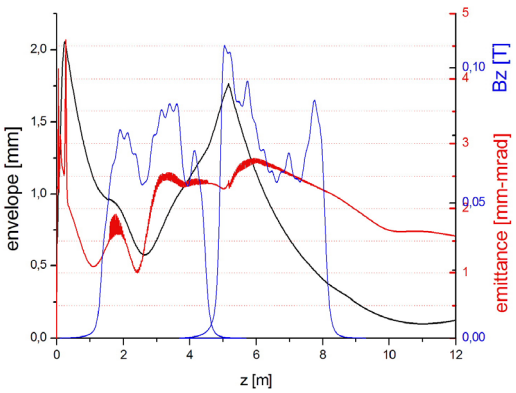

Figure 6: Envelope (left axis), emittance (right axis) and the magnetic field profile (right axis) vs z (m).

The injection angle and the characteristics of the beam are presented in Table 3.

The analysis on the phase space shows that the current profile is much more peaked than a Gaussian function. A fitting process permits to argue that only about 30 % of the charge concentrated in a slice of about 20 μm contributes to the emission. With these values of charge and width, the beam turns out to be in a condition producing radiation with 1 or 2 spikes.

The difference between the cases at low charge and the operation at high charge is substantially in the total energy extracted, that in this last case achieves 1.4 mJ, two order of magnitude larger than the low charge cases. The other parameters, as the radiation duration, divergence and bandwidth are comparable. All the radiation parameters are presented in Table IV. The radiation level curves in the plane (s,z), together with the pulse shape at 4 meters are presented in Fig. 7 .

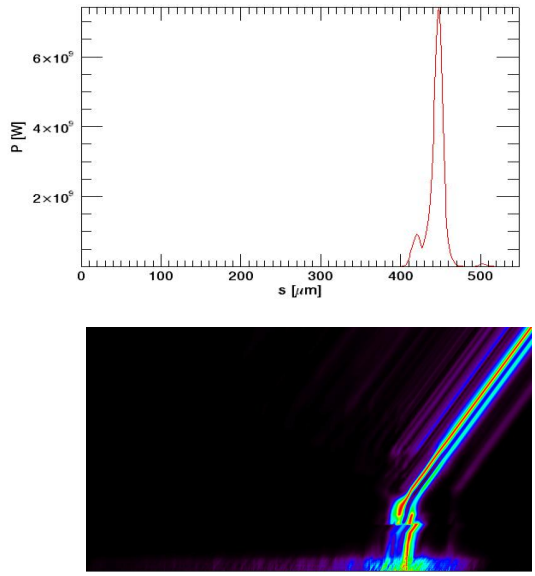

Figure 7: σ_x =100 μm: pulse shape P (W) vs s(μm) at z= 4 m. Normalized level curves in the plane z(m) vs s (μm).

CONCLUSIONS

The production of single spike, clean pulse of radiation in the SPARC device at 500 nm has been analysed in both low and high charge operation regimes. The velocity bunching method of compression allows to obtain bunches with very much peaked profiles. In this way, only the part of the charge in the higher current slices contributes to the radiation emission. The radiation pulse is short and single spiked, the energy yield ranging between few tens of μJ in the low charge regime to few mJ in the high charge regime.

REFERENCES

[1] R. Bonifacio et al. PRL 73 (1994) 70
[2] J. Rosenzweig et al. NIMA 593, 45 (2008)
[3] M.Boscolo et al, NIMA 593 137 (2008)
[4] M. Xie in Proc. of the 1995 PAC, IEEE, Piscataway, NJ,1995, p.183
[5] M. Ferrario et al. PRL 99 (2007) 234801
[6] M. Boscolo et al.: SPARC BD-note BD-07-006
[7] L.M. Young, LANL Report No.LA-UR-96-1835
[8] K. Floetmann, ASTRA: http://desy.de/~mpyflo/Astra_dokumentation/
[9] A. Bacci et al., NIMB 263 (2007) 488
[10] S. Reiche: NIM A 429 (1999) 243